Rifabutin is bactericidal against intracellular and extracellular forms of Mycobacterium abscessus

Matt D Johansen, Wassim Daher, Françoise Roquet-Banères, Clément Raynaud, Matthéo Alcaraz, Florian P Maurer, Laurent Kremer

Rifabutin is bactericidal against intracellular and extracellular forms of *Mycobacterium abscessus*

Matt D. Johansen[1], Wassim Daher[1,2], Françoise Roquet-Banères[1], Clément Raynaud[1], Matthéo Alcaraz[1], Florian P. Maurer[3,4], and Laurent Kremer[1,2,#]

[1]Centre National de la Recherche Scientifique UMR 9004, Institut de Recherche en Infectiologie de Montpellier (IRIM), Université de Montpellier, 1919 route de Mende, 34293, Montpellier, France.

[2]INSERM, IRIM, 34293 Montpellier, France.

[3]National and WHO Supranational Reference Center for Mycobacteria, Research Center Borstel-Leibniz Lung Center, 23845 Borstel, Germany.

[4]Institute of Medical Microbiology, Virology and Hygiene, University Medical Center Hamburg-Eppendorf, Hamburg, Germany

[#]To whom correspondence should be addressed:

Tel: (+33) 4 34 35 94 47; E-mail: laurent.kremer@irim.cnrs.fr

Running title: *In vivo* efficacy of rifabutin against *M. abscessus*

Keywords: *Mycobacterium abscessus*, rifabutin, macrophage, zebrafish, therapeutic activity.

ABSTRACT

Mycobacterium abscessus is increasingly recognized as an emerging opportunistic pathogen causing severe lung diseases. As it is intrinsically resistant to most conventional antibiotics, there is an unmet medical need for effective treatments. Repurposing of clinically validated pharmaceuticals represents an attractive option for the development of chemotherapeutic alternatives against *M. abscessus* infections. In this context, rifabutin (RFB) has been shown to be active against *M. abscessus* and has raised renewed interest in using rifamycins for the treatment of *M. abscessus* pulmonary diseases. Herein, we compared the *in vitro* and *in vivo* activity of RFB against the smooth and rough variants of *M. abscessus*, differing in their susceptibility profile to several drugs and physiopathologial characteristics. While the activity of RFB is greater against rough strains than in smooth strains *in vitro*, suggesting a role of the glycopeptidolipid layer in susceptibility to RFB, both variants were equally susceptible to RFB inside human macrophages. RFB treatment also led to a reduction in the number and size of intracellular and extracelluar mycobacterial cords. Furthermore, RFB was highly effective in a zebrafish model of infection and protected the infected larvae from *M. abscessus*-induced killing. This was corroborated with a significant reduction in the overall bacterial burden, as well as decreased numbers of abscesses and cords, two major pathophysiological traits in infected zebrafish. This study indicates that RFB is active against *M. abscessus* both *in vitro* and *in vivo,* further supporting its potential usefulness as part of combination regimens targeting this difficult-to-treat mycobacterium.

INTRODUCTION

Nontuberculous mycobacteria (NTM) are environmental mycobacteria. Among all NTM, *Mycobacterium avium* and *Mycobacterium abscessus* represent the most frequent pathogens associated with pulmonary disease (1). *M. abscessus* is a rapidly growing NTM of increasing clinical significance, particularly in cystic fibrosis (CF) patients (2). In CF patients, infection with *M. abscessus* correlates with a more rapid decline in lung function and can represent an obstacle to subsequent lung transplantation (3–5). From a taxonomical view, the species currently comprises three subspecies: *M. abscessus* subsp. *abscessus* (designated hereafter *M. abscessus)*, *M. abscessus* subsp. *bolletii* (designated hereafter *M. bolletii)* and *M. abscessus* subsp. *massiliense* (designated hereafter *M. massiliense*) (6). These subspecies exhibit different clinical outcomes and drug susceptible profiles to antibiotic treatments (7).

M. abscessus strains can exhibit either a smooth (S) or rough (R) morphotype as a consequence of the presence or absence, respectively, of bacterial surface glycopeptidolipids (GPL) (1, 8–10). These morphological distinctions are associated with important physiological differences. S variants are more hydrophilic than R variants, enabling increased sliding motility and the capacity to form biofilms (8, 9, 11), while the aggregative R variants possess a high propensity to produce large bacterial cords (11, 12). While S and R variants can be viewed as two representatives of the same isolate, which can co-exist and evolve differently in response to host immunity, they express different pathophysiological traits (10). S variants are typically less virulent than the R variants (11, 13, 14), the latter being more frequently associated with severe lung diseases and persisting for years in CF patients (3, 5). Importantly, an S-to-R transition within the colonized host (5, 15) is linked to genetic polymorphisms within the GPL biosynthetic/transport locus (15, 16). Moreover, differences in the susceptibility to drug candidates have been identified between S and R variants (17, 18), highlighting the need for the improved evaluation of new compounds/drug regimens against both morphotypes.

Treatment of *M. abscessus* lung disease remains particularly challenging, largely due to intrinsic resistance to wide panel of antimicrobial agents, including most antitubercular drugs such as rifampicin (RIF) (19–22). The extensive resistome of *M. abscessus* results from a low permeability of the cell wall, absence of drug-activating systems, induction of efflux pumps and production of a wide panel of drug-modifying enzymes (19, 22, 23). In addition, mutations in genes encoding drug targets

79 can result in acquired drug resistance further complicating therapy (1, 24). Treatment of infections
80 caused by *M. abscessus* require prolonged courses of multiple antibiotics, usually combining a
81 macrolide (azithromycin or clarithomycin), a β-lactam (imipenem or cefoxitin) and an aminoglycoside
82 (amikacin) (25, 26, 27). Additional drugs, such as tigecycline or clofazimine, are often added to
83 strengthen the regimen, particularly in response to toxic side effects or unsatisfactory clinical
84 response (28). Despite intensive chemotherapy, treatment success rates typically remain around 25-
85 40% in the case of macrolide resistance, which occurs in at least 40-60% of clinical isolates (29).
86 Therefore, there is an urgent clinical need for new drug regimens with improved efficacy (30). While
87 the current drug pipeline against *M. abscessus* remains poor, it has recently been fueled with the
88 discovery of several active hits and the development of repurposed drugs (24). Among the latter,
89 screening of libraries of approved pharmaceuticals revealed that rifabutin (RFB), a rifamycin related
90 to the poorly active rifampicin (RIF), shows activity against *M. abscessus* (31, 32). RIF, along with
91 many other rifamycins, is inactivated by the ADP-ribosyltransferase (Arr_{Mab}) encoded by *MAB_0591*,
92 which ribosylates the drug at the C23 hydroxyl position (33). RFB has also been reported to be as
93 active as clarithromycin in immune-compromized NOD/SCID mice infected with *M. abscessus* (34).
94 However, most studies on RFB have been carried out on either S or R variants (when reported),
95 rendering results sometimes difficult to interpret and/or to compare. Due to the co-existence of S
96 and R variants in patients (15) and the presence of each variant in different compartments (S residing
97 mostly in macrophages and R growing also in the form of intra- or extracellular cords), it is essential
98 to address the activity of RFB on isogenic S/R pairs in both *in vitro* and *in vivo* studies.
99 The present study aimed to describe and compare the activity of RFB against S and R *M.*
100 *abscessus* complex strains *in vitro* and *ex vivo* in a macrophage infection model. Due to the
101 importance of cording, considered as a marker of severity of the infection with the R variant, we also
102 investigated the efficacy of RFB in a zebrafish model of infection.

MATERIALS AND METHODS

Mycobacterial strains and growth conditions. *M. abscessus* CIP104536^T, *M. bolletii* CIP108541^T and *M. massiliense* CIP108297^T reference strains and clinical isolates from CF and non-CF patients were reported previously (35, 36). Strains were routinely grown and maintained at 30°C in Middlebrook 7H9 broth (BD Difco) supplemented with 0.05% Tween 80 (Sigma-Aldrich) and 10% oleic acid, albumin, dextrose, catalase (OADC enrichment; BD Difco) (7H9$^{T/OADC}$) or on Middlebrook 7H10 agar (BD Difco) containing 10% OADC enrichment (7H10^{OADC}) and in the presence of antibiotics, when required. For drug susceptibility testing, bacteria were grown in Cation-Adjusted Mueller-Hinton Broth (CaMHB; Sigma-Aldrich). RFB was purchased from two independent commercial sources (Adooq Bioscience and Selleckchem) and dissolved in DMSO.

Drug susceptibility testing. The minimal inhibitory concentrations (MIC) were determined according to the CLSI guidelines (37). The broth micro-dilution method was used in CaMHB with an inoculum of $5x10^6$ CFU/mL in exponential growth phase. The bacterial suspension was seeded in 100 µL volumes in all of the wells of a 96-well plate, except for the first column, to which 198 µL of the bacterial suspension was added. In the first column, 2 µL of drug at its highest concentration was added to the first well containing 198 µL of bacterial suspension. Two-fold serial dilutions were then carried out and the plates were incubated for 3-5 days at 30°C. MICs were recorded by visual inspection. Assays were completed in triplicate in three independent experiments.

Growth inhibition kinetics. To monitor growth inhibition of *M. abscessus* CIP104536^T S and R, 96-well plates were set-up as for MIC determination and serial dilutions of the bacterial suspensions exposed to increasing concentrations of RFB were plated on LB agar plates after 0, 24, 48 and 72 hrs. Colony-forming units (CFUs) were counted after 4 days of incubation at 30°C. Results from each drug concentration are representative of at least 2 independent experiments.

Cytotoxicity assay. THP-1 cells were differentiated with PMA for 48 hrs and exposed to decreasing concentrations of either RFB or RIF (starting at 200 µg/mL) for an additional 72 hrs at 37°C with 5% CO_2. Following incubation, 10% (vol/vol) resazurin dye was added to each well and left to incubate for

4 hrs at 37°C and 5% CO_2. Data was acquired using a fluorescent plate reader (excitation 540 nm, emission 590 nm). DMSO was included as a negative control, while SDS was included as a positive control.

Intracellular killing assay. Human THP-1 monocytes were grown in RPMI medium supplemented with 10% Fetal bovine serum (Sigma Aldrich) ($RPMI^{FBS}$) and incubated at 37°C in the presence of 5% CO_2. Cells were differentiated into macrophages in the presence of 20 ng/mL Phorbol Myristate Acetate (PMA) in 24-well flat-bottom tissue culture microplates (10^5 cells/mL) and incubated for 48 hrs at 37°C with 5% CO_2. Infection with clinical isolates or *M. abscessus* harbouring pTEC27 fluorescent tdTomato was carried out at 37°C in the presence of 5% CO_2 for 3 hrs at a MOI 2:1. After extensive washing with 1X phosphate buffered saline (PBS), cells were incubated with $RPMI^{FBS}$ containing 250 µg/mL amikacin for 2 hrs and washed again with PBS prior to the addition of 500 µL $RPMI^{FBS}$ containing DMSO (negative control) or 500 µL $RPMI^{FBS}$ containing 50 µg/mL of RIF or AMK, or 12.5 µg/mL of RFB. Macrophages were washed with PBS and lysed with 100 µL of 1% Triton X-100 at required time points. Serial dilutions of macrophage lysates were plated onto LB agar plates and colonies were counted to determine intracellular CFUs.

Microscopy-based infectivity assays. Monocytes were differentiated into macrophages (THP-1) in the presence of PMA and were grown on coverslips in 24-well plates at a density of 10^5 cells/mL for 48 hrs at 37°C with 5% CO_2 prior to infection with Tdtomato expressing *M. abscessus* for 3 hrs at a MOI of 2:1. After washing and AMK treatment to remove the extracellular bacilli, macrophages were exposed to DMSO (negative control), or 50 µg/mL RIF or AMK, or 12.5 µg/mL RFB, and fixed at 0, 1 and 3 days post-infection with 4% paraformaldehyde in PBS for 20 min. Cells were then permeabilized using 0.2% Triton X-100 for 20 min, blocked with 2% BSA in PBS supplemented with 0.2% Triton X-100 for 20 min, incubated with anti-CD63 antibodies (Becton Dickinson); dilution 1:1000) for 1 hr and with an Alexa Fluor 488-conjugated anti-mouse secondary antibody (Molecular Probes, Invitrogen). After 5 min of incubation with DAPI (dilution 1:1000), cells were mounted onto microscope slides using Immu-mount (Calbiochem) and examined with an epifluorescence microscope using a 63X objective. The average proportion of macrophages containing fewer than <5, 5-10, or >10 bacilli were quantified using Zeiss Axio-vision software. Images were acquired by

focusing on combined signals (CD63 in green and red fluorescent *M. abscessus*) and captured on a Zeiss Axio-imager confocal microscope equipped with a 63X oil objective and processed using Zeiss Axiovision software. Quantification and scoring of the numbers of bacilli present within macrophages were performed using ImageJ. Equal parameters for the capture and scoring of images were consistently applied to all samples. For each condition, approximately 1000 infected macrophages were analyzed. The presence of the intra- or extracellular cords within or among the macrophages infected with the R morphotype strain were treated in the presence of DMSO, RIF, RFB or AMK at the concentrations previously described, counted and imaged using confocal microscopy.

Assessment of RFB efficacy in infected zebrafish. Experiments in zebrafish were conducted according to the Comité d'Ethique pour l'Expérimentation Animale de la Région Languedoc Roussillon under the reference CEEALR36-1145. Experiments were performed using the *golden* mutant (38). Embryos were obtained and maintained as described (14). Embryo age is expressed as hours post fertilisation (hpf). Red fluorescent *M. abscessus* CIP104536^{T} (R) expressing tdTomato were prepared and microinjected in the caudal vein (2-3 nL containing ≈100 bacteria/nL) in 30 hpf embryos previously dechorionated and anesthetized with tricaine, as described earlier (39). The bacterial inoculum was checked *a posteriori* by injection of 2 nL in sterile PBS^{T} and plating on 7H10^{OADC}. Infected embryos were transferred into 24-well plates (2 embryos/well) and incubated at 28.5°C to monitor kinetics of infection and embryo survival. Survival curves were determined by counting dead larvae daily for up to 12 days, with the experiment concluded when uninfected embryos started to die. RFB treatment of infected embryos and uninfected embryos was commenced at 24 hpi (hours post-infection) for 4 days. The drug-containing solution was renewed daily. Bacterial loads in live embryos were determined by anesthetising embryos in tricaine as previously described (40), mounting on 3% (w/v) methylcellulose solution and taking fluorescent images using a Zeiss Axio Zoom.V16 coupled with an Axiocam 503 mono (Zeiss). Fluorescence Pixel Count (FPC) measurements were determined using the 'Analyse particles' function in ImageJ (39). Bacterial cords were identified based on the size and shape of fluorescent bacteria within the live zebrafish embryo, vastly exceeding the surrounding size and shape of neighbouring cells. All experiments were completed at least three times independently.

Overexpression of *MAB_1409c* in *M. abscessus*.

Overexpression was achieved by PCR amplification of *MAB_1409c* (*tap)* in fusion with an HA tag using genomic DNA and the forward primer (5'- gagaCAATTGCCATGTCCACTCCGACGGCGGATTC-3'; MfeI) and reverse primer (5'-gagaGTTAACCTAAGCGTAATCTGGAACATCGTATGGGTACCGAGTTGGTTCCTTGTCGGGCT-3'; HpaI). The amplified product was digested with MfeI/HpaI and ligated into the MfeI/HpaI-restricted pMV306 integrative vector to generate pMV306-*MAB_1409c*-HA where *MAB_1409c-HA* is under the control of the *hsp60* promoter. The construct was sequenced and electroporated in *M. abscessus* S and R.

Selection of resistant *M. abscessus* mutants and target identification. Exponentially growing *M. abscessus* CIP104536^T R cultures were plated on LB agar containing either 25 or 50 µg/mL RFB. After one week of incubation at 37°C, four individual colonies from each RFB concentration were selected, grown in CaMHB, individually assessed for MIC determination and scored for resistance to RFB. Identification of SNPs in the resistant strains was completed by PCR amplification using *rpoB_f* 5'-TCAGTGGGGCTGGTTAG -3' and *rpoB_r* 5'-AAAACATCGCAGATGCGC-3' to produce a 3541 bp amplicon for full coverage sequencing of the *rpoB* gene.

Western blotting. Bacteria were harvested, resuspended in PBS, and disrupted by bead-beating with 1-mm diameter glass beads. The protein concentration in the lysates was determined and equal amounts of proteins (100 µg) were subjected to SDS/PAGE. Proteins were transferred to a nitrocellulose membrane. For detection of Tap-HA and KasA (loading control), the membranes were incubated for 1 hr with either the rat anti-HA or rat anti-KasA antibodies (dilution 1:2000), washed, and subsequently incubated with goat anti-rat antibodies conjugated to HRP (Abcam, dilution 1:5000). The signal was revealed using the ChemiDoc MP system (Bio-Rad).

Statistical analyses. Statistical analyses were performed on Prism 5.0 (Graphpad) and detailed for each figure legend. *$P \leq 0.05$, ** $P \leq 0.01$, *** $P \leq 0.001$, **** $P \leq 0.0001$.

RESULTS

Rough *M. abscessus* is more susceptible to RFB treatment than smooth *M. abscessus in vitro*. Exposure of exponentially-growing *M. abscessus* CIP104536^T S and R isogenic variants to increasing concentrations of RFB, starting at 25 µg/mL for S and 6.25 µg/mL for R, resulted in a noticeable growth inhibition **(Fig. 1)**. At the lowest concentration, the CFUs at 72 hrs post-treatment remained comparable to those of the inoculum, suggestive of a bacteriostatic effect. However, the highest RFB concentrations for both S (200 µg/mL) and R (50 µg/mL) variants were accompanied by 1.81 and 2.47 Log reduction in the CFU counts at 72 hrs post-treatment, respectively **(Fig. 1)**. While similar bactericidal effects of RFB were observed against both variants, this was achieved with lower concentrations of RFB against the R variant relative to the isogenic S variant. Overall, RFB at concentratios of 12.50 µg/mL (For R) resulted in a killing effect comparable to the one of imipenem (IPM) used at the MIC (16 µg/mL), known as an active β-lactam drug against *M. abscessus* (41) **(Fig. 1)**.

To confirm the differences in the susceptibility to RFB, we determined the MIC of the CIP104536^T S and R variants in CaMHB. **Table 1** clearly shows that the S strain is 4-fold more resistant than its R counterpart. However, both variants were similarly resistant to other rifamycins (RIF, RPT and RFX), in agreement with previous studies (32, 34). Our MIC values, obtained in repetitive experiments with two different commercial sources of RFB, were higher than those reported earlier (32, 34), but comparable to values reported in another study (42). Consistently with other studies (31), we also noticed that the MIC values were dependent on the culture medium **(Table S1)**. Interestingly, MICs of RFB against S and R strains were lower in Middlebrook 7H9 as compared to CaMHB but this effect was lost when supplementing the medium with OADC enrichment. In contrast the S and R strains displayed equal susceptibility levels to RFB in Sauton's medium.

To investigate the relationship between RFB activity and GPL production, drug susceptibility was assessed in CaMHB using the GPL-deficient Δ*mmpL4b* mutant, generated in the S background of the type strain CIP104536^T, and its complemented counterpart (14, 43, 44). The *mmpL4b* gene encodes the MmpL4b transporter which participates in the translocation of GPL across the inner membrane (43, 45). Mutations in this gene are associated with loss of GPL and acquisition of a R morphotype

(13, 43). The parental S strain and, to a lesser extent the Δ*mmpL4b*-complemented strain, showed reduced susceptibility to RFB (MIC 32-64 μg/mL) than the *M. abscessus* R strain and the GPL-deficient Δ*mmpL4b* mutant (MIC 16 μg/mL) **(Table 1)**. The MIC results are in agreement with the growth inhibition kinetics **(Fig. 1)** and suggest that the outer GPL layer influences the activity of RFB.

M. abscessus possesses numerous potential drug efflux systems (45), including MAB_1409c, a homolog of Rv1258c, previouly reported to mediate efflux of RIF in *M. tuberculosis* (46). We thus addressed whether overexpression of MAB_1409c induces resistance to RFB in *M. abscessus*. *MAB_1409c* was cloned in frame with a HA-tag in the integrative pMV306. The resulting construct pMV306-*MAB_1409c*-HA was introduced in both S and R variants and the expression of MAB_1409c was confirmed by Western blot analysis using anti-HA antibodies **(Fig. S1)**. Drug susceptibility assessment indicated a 4-fold upshift in the MIC of RFB against the R strain carrying pMV306-*MAB_1409c*-HA while no changes in the MIC were observed with the S strain overproducing MAB_1409c **(Table 1)**. This suggests that increasing expression of MAB_1409c in the R variant is likely to mediate efflux of RFB, leading to reduced susceptibility to the drug.

RFB is active against S and R *M. abscessus* isolates *in vitro*. The activity of RFB was next tested using a set of clinical strains isolated from CF patients or non-CF patients. In general, the MIC of R strains were 2 to 4 times lower than those of S strains, altough there were variations among the strains **(Table 2)**. Some R strains (10, 112, 179, 210) exhibited higher MIC values (100 μg/mL) than the reference CIP104536^T R strain, while one S strain appeared particularly susceptible to RFB (*M. massiliense* 120 with a MIC of 6.25 μg/mL). These differences between strains and S/R morphotypes were not observed previously with BDQ and S and R variants were also equally sensitive to BDQ (47). Overall, these results demonstrate that RFB is active against *M. abscessus*, including isolates from CF patients, while R variants appear in general more susceptible to RFB than S variants, supporting previous findings (48).

Mutations in *rpoB* confer resistance to RFB. Although rifamycin resistance mechanisms mediated by mutations in the *rpoB* gene coding for the β-subunit of RNA polymerase have been widely described for *M. tuberculosis*, this is not the case for *M. abscessus*. Therefore, to identify the mechanism of

resistance of RFB, a genetic approach involving the selection of spontaneous RFB-resistant mutants of *M. abscessus* followed by *rpoB* sequencing was applied. Four spontaneous strains were isolated in the presence of 25 or 50 µg/mL RFB, exhibiting 4- to 8-fold increased resistance levels as compared to the parental strain, respectively **(Table 3)**. Sequencing analyses of *rpoB* identified several single nucleotide polymorphisms (SNPs) across four resistor mutants. In mutants 25.1 and 50.1, a C1339T substitution was identified at position 447 (H447Y). Similarly, in mutant 25.2, a C1339G replacement was found, resulting in an amino acid substitution at position 447 (H447D). Comparatively, in mutant strain 50.2, another SNP (C1355T) occurred, leading to an amino acid change at position 452 (S452L). A comparison of growth of different resistant strains on agar plates containing increasing concentrations of RFB is shown in **Fig. S2**. Whereas RFB abrogated growth of the wild-type S and R strains, growth of all four resistors harbouring mutations at either positions 447 or 452 sustained bacterial growth at 50 µg/mL, confirming that mutations in *rpoB* confer resistance to RFB.

***M. abscessus* S and R strains are equally susceptible to RFB in macrophages.** While RFB has been shown to be active against *M. tuberculosis* in a macrophage infection model (49), this has not been thoroughly investigated for *M. abscessus*. We thus compared the intracellular efficacy of RFB in THP-1 macrophages infected with either S or R variants. Firstly, the cytotoxicity of RFB and RIF against THP-1 cells was investigated over a 3-days exposure period to either drug. **Fig. S3**, clearly shows that RFB exerts significant cytotoxicity at concentration >25 µg/ml and that the kinetic of macrophage killing was more rapid with RFB than with RIF. Based on these results, all subsequent macrophage studies were treated with 50 µg/mL RIF or 12.5 µg/mL RFB. AMK at 50 µg/mL was added as a positive control. DMSO-treated macrophages were included as a negative control for intracellular bacterial replication. At 0, 1 and 3 days post-infection (dpi), macrophages were lysed and plated to determine the intracellular bacterial loads following drug treatment. Whereas the presence of DMSO or RIF failed to inhibit intramacrophage growth of *M. abscessus* S, exposure to RFB strongly decreased the intracellular bacterial loads at 1 dpi, with this effect further exacerbated at 3 dpi **(Fig. 2A)**. As anticipated, treatment with RIF did not show any effect, in agreement with the poor activity of this compounds *in vitro* **(Table 1)**. Comparatively, AMK treatment resulted in a significantly reduced intracellular growth rate in both *M. abscessus* S and R variants between 1 and 3dpi. Interestingly, the

RFB susceptibility profile for the S variant at 1 and 3 dpi was comparable to that of the R variant, with a ~3 Log reduction in the CFU counts **(Fig. 2A and B**, respectively**)**.

Macrophages were next infected with *M. abscessus* strains expressing Tdtomato and exposed to either DMSO, AMK, RIF or RFB, followed by staining with anti-CD63 and DAPI and observed under a confocal microscope. A quantitative analysis confirmed the marked reduction in the number of *M. abscessus* S-infected THP-1 cells treated with AMK and RFB at 1 and 3 dpi compared to RIF-treated cells or untreated control cells **(Fig. 2C)**. A similar trend was observed when macrophages were infected with *M. abscessus* R **(Fig. 2D)**.

Macrophages infected with the S variant were then classified into three categories based on their bacterial burden: poorly infected (<5 bacilli), moderately infected (5-10 bacilli) and heavily infected (>10 bacilli) macrophages. Cells containing bacilli were then individually observed under the microscope and scored to one of the three categories. The quantitative analysis indicates that exposure to RFB significantly reduces the percentage of S variant heavily infected THP-1 cells while increasing the proportion of the poorly infected category, as compared to the untreated cells at 1 dpi **(Fig. 2E)**. At 3 dpi, the effect of RFB was even more pronounced with 10% of the infected bacilli belonging to the heavily infected category and more than 50% associated with the poorly infected category. Analysis performed on cells infected with the R variant generated a similar category profile, although treatment with RFB was associated with a higher proportion of heavily infected macrophages at 3 dpi with the R variant than with the S variant **(Fig. 2F). Fig. 2G** illustrates the reduced number of *M. abscessus* S in infected THP-1 cells treated with RFB at 1 dpi, as compared to the untreated control cells (DMSO) or those treated with RIF or AMK. Collectively, these results indicate that RFB enters THP-1 macrophages and similarly impedes bacterial replication of both *M. abscessus* S and R variants.

RFB reduces the intramacrophage growth of clinical isolates. RFB has recently shown vast potential as an effective antibiotic for the treatment of *M. abscessus* infection in a NOD/SCID murine model (34). However, to date the efficacy of RFB has only been evaluated against a limited panel of *M. abscessus* clinical isolates within an infection setting. As such, we explored the activity of RFB against S and R clinical isolates of the *M. abscessus* complex with varying MIC values against RFB within THP-1 macrophages. In support of our previous findings in infected macrophages, RFB treatment (12.5 or

25 µg/mL) was very active against all *M. abscessus* subspecies within macrophages at 1 and 3 dpi when compared to Day 0 and DMSO treatment **(Fig. 3)**, irrespective of S and R morphotypes and the corresponding MIC values **(Table 2)**. Overall, these findings suggest that RFB is very effective against intracellular clinical isolates and highlights the lack of direct correlation between MICs determined *in vitro* and the intracellular activity of RFB.

Reduced intra- and extracellular cording by RFB treatment. An important phenotypic difference between S and R morphotypes is that R morphotypes display increased bacterial aggregation. R bacilli remain attached during replication, forming compact colonies containing structures that resemble cords on agar and in broth medium (8, 12, 14). **Fig. 4A** clearly shows that, upon infection with *M. abscessus* R expressing TdTomato, the total number of cords per field was significantly reduced in the presence of 50 µg/mL AMK or 12.5 µg/mL RFB when compared to 50 µg/mL RIF or DMSO alone. Moreover, we observed intracellular cords that are capable of growing inside the macrophage as well as in the extracellular milieu, which were easily observable at 3 dpi (**Fig. 4B**). As illustrated in **Fig. 4C**, treatment with AMK or RFB strongly impacted on both intra- and extracellular cords. While AMK treatment severely reduced the number of both intra- and extracellular cords, this effect was almost completely abrogated with RFB at 3 dpi. Together, these results indicate that RFB is highly effective in reducing *M. abscessus* cords, thought to affect the outcome of the infection.

RFB treatment enhances protection of zebrafish infected with *M. abscessus*. *In vivo* drug efficacy has previously been well described using the zebrafish model of infection (40, 47, 50). Initial experiments indicated that RFB concentrations ≤ 100 µg/mL (final concentration in fish water) did not interfere with larval development and was well tolerated in embryos when treatment was applied for 4 days with daily drug renewal **(Fig. 5A)**. Higher concentrations of RFB, however, were associated with rapid larval death. As such, only lower RFB doses (≤ 100 µg/mL) were used in subsequent studies. Red fluorescent tdTomato-expressing *M. abscessus* (R variant) was microinjected in the caudal vein of embryos at 30 hrs post-fertilisation (hpf). RFB was directly added at 1 dpi to the water containing the infected embryos, with RFB-supplemented water changed on a daily basis for 4 days. Embryo survival was monitored and recorded daily for 12 days. No decrease in the survival rate was observed in the presence of 5 µg/mL RFB, however, a significant dose-dependent increase in the

survival of embryos exposed to 25 or 50 µg/mL RFB was observed as compared to the untreated group **(Fig. 5B)**. When exposed to 50 µg/mL RFB, the highest dose examined in this setting, nearly 80% of the treated embryos survived at 12 dpi, as compared to 40% of the untreated group. This clearly indicates that RFB protects zebrafish from *M. abscessus* infection.

To test whether RFB exerts an effect on the bacterial burden in zebrafish, we quantified fluorescent pixel counts (FPC) (39). As expected, embryos treated with 50 µg/mL RFB had significantly decreased bacterial burdens at 2, 4 and 6 dpi when compared to the untreated group (**Fig. 5C**). These results were corroborated by imaging whole embryos, characterised by the presence of large abscesses and cords in the brain when left untreated and which were observed much less frequently in the RFB-treated animals despite the presence of single bacilli or small aggregated bacteria **(Fig. 5D)**.

RFB treatment reduces abscess formation by *M. abscessus* in zebrafish. Virulence of *M. abscessus* R variants in zebrafish are correlated with the presence of abscesses, particularly in the central nervous system (14, 39). To address whether the enhanced survival of RFB-treated fish is associated with decreased abscess formation, the percentage of abscesses and cords were determined by monitoring abscesses and cords in whole embryos, as reported previously (14, 39). Extracellular cords can be easily distinguished based on their serpentine-like shape and by their size, often greater as compared to the size of the surrounding macrophages and neutrophils. Exposure of infected embryos to 50 µg/mL RFB was accompanied by a significant decrease in the proportion of embryos with cords **(Fig. 6A)** at 4 dpi, and the number of embryos with abscesses **(Fig. 6B)** at 4 and 6 dpi. This decrease in the physiopathological signs of RFB-treated larvae correlates also with the FPC analysis and whole embryo imaging **(Fig. 6C and 6D)**. Overall, these results demonstrate that RFB reduces the pathophysiology of *M. abscessus* infection in zebrafish larvae and protects them from bacterial killing.

DISCUSSION

Treatment success of infections caused by *M. abscessus* is unacceptably low even upon prolonged, multidrug chemotherapy with a significant risk of severe toxic side effects. Although RIF is used as a first-line drug against *M. tuberculosis*, it has no activity against *M. abscessus*. While ADP ribosyltransferases can utilise both RIF and RFB as substrates (51), a lower catalytic efficiency with RFB may explain its greater potency against *M. abscessus*. Our study supports and extends previous investigations highlighting the potential of RFB against *M. abscessus in vitro* against a wide panel of *M. abscessus* complex clinical isolates (31, 32, 52, 53). We found, however, that our MIC values were higher than those observed in previous investigations (31, 32). In our study, following the Clinical and Laboratory Standard Institute (CLSI) guidelines, MIC were determined in CaMHB while Aziz *et al*. showed that MIC values were 2- to 3-fold higher in CaMHB as compared to Middlebrook 7H9 (31), clearly implicating an effect of medium on RFB susceptibility testing. In line with these results, we noticed important variations in the MIC values depending on the culture medium used for RFB susceptibility assessments. It is also noteworthy that the growth curve of the untreated S strain is different from the one of the R strain, which is very likely linked to the highly aggregative surface properties typifying the R strain which, in contrast to the S strain, produces very clumpy and corded cultures in broth medium (10, 39, 54). As a consequence, colonies on agar plates are very likely emerging from aggregated bacteria rather than individual bacilli, explaining why the CFU counts were significantly lower in both cultures. Thus, the CFU counts of the R strain does not accurately reflect the absolute number of living bacilli in the culture. We also selected RFB-resistant mutants and identified mutations in *rpoB,* known as the primary target of rifampicin in *M. tuberculosis* (55). Interestingly, the mutations identified are part of the rifampicin-resistance-determining region (RRDR), a 81-bp central segment corresponding to codons 426 to 452 in *M. tuberculsosis* that harbours the vast majority of *rpoB* mutations associated with resistance to RIF (55). Noteworthingly, S452L corresponds to one of the most frequently mutated coding region in the *rpoB* gene in *M. tuberculosis* (S450L replacement) (55). Together, these results suggest RpoB is very likely the target of RFB in *M. abscessus*.

Among the various studies reporting the activity of RFB against *M. abscessus in vitro*, very few discriminated the activity of RFB against the S or R morphotypes. Herein, we found that the type

strain CIP104536^T S was reproducibly more resistant to RFB than its R counterpart. Supporting these results, deletion of *mmpL4b* in the S genetic background, resulting into an R morphotype lacking GPL (13, 43), increased susceptibility to RFB. Conversely, functional complementation of the *mmpL4b* mutant, restoring the S morphotype and GPL production (13, 43), partially rescued the higher MIC. This highlights the influence of the outermost GPL layer on susceptility to RFB. Previously, the activity of other inhibitors have been shown to be dependent on the presence or absence of GPL in *M. abscessus* (17, 18). A logical explanation is that the GPL layer protects the bacilli from the penetration of drugs. The absence of GPL may enhance the permeability of the cell wall and accumulation of the drug inside the bacteria. However, one cannot exclude the possibility that MmpL4b, like other MmpL transporters, can act as an efflux pump (56–58) and may participate in the extrusion of RFB in *M. abscessus* S, resulting in higher MIC. The implication of efflux pumps in resistance to RFB has been investigated, whereby the overexpression of MAB_1409c (a homologue of the *M. tuberculosis* Rv1258c) resulted in increased resistance to RFB in the R variant of *M. abscessus*. This effect was not observed in the S strain overexpressing MAB_1409c, presumably because of the already elevated MIC of the parental S strain towards RFB. However, while the increased susceptibility of the R strain as compared to the S strain was true with respect to the type strain, this was not observed for all clinical strains tested. The heterogeneity of the clinical strains in response to RFB treatment cannot be simply explained by the presence or absence of GPL, but may also include additional determinants of resistance to RFB (52), such as differences in the expression level of Arr_{Mab} or the expression of Rox monooxygenases, known to inactivate RIF in other bacterial species as proposed earlier (59). This, however, requires further investigation in follow-up studies.

One unanticipated finding from this study relies on the fact that, although S and R variants respond differently to RFB treatment *in vitro*, this was not the case against the intracellularly-residing *M. abscessus*. We found that, using a macrophage model of infection, the isogenic S and R type strains responded equally well to treatment with 12.5 µg/mL RFB, largely exceeding the results obtained with AMK, a drug displaying weak intracellular activity (60). These observations are reminiscent of other studies indicating that various naphtalenic ansamycins, including RIF, differ profoundly in their capacity to kill extracellular *Staphylococcus aureus*, albeit there were few differences observed between them in promoting human macrophages to kill phagocytosed bacteria (61). There is no simple explanation as why *M. abscessus* S is as efficiently killed as *M. abscessus* R

inside the cells. A plausible explanation may be that the stress response inside macrophages alters the composition/architecture of the cell wall of *M. abscessus*, thereby affecting the GPL layer and/or permeability of the S variant. It has been shown that the GPL layer significantly influences the hydrophobic surface properties (62), potentially impacting on the adhesion and the uptake of the bacilli. Furthermore, electron microscopy observations revealed that the electron translucent zone (ETZ) that fills the entire space between the phagosome and the bacterial surface relies on GPL production in the S variant (11). Alternatively, RFB may directly induce the antimycobacterial activity of the macrophage, which in turns translates into a rapid killing of the phagocytosed bacteria, regardless of their morphotype. Overall, these results suggest that the MIC values of RFB are not indicative of the intraphagocytic killing of *M. abscessus* and highlights the importance of testing the efficacy of drugs in a macrophage infection model.

Cords and abscesses are pathophysiological markers of *M. abscessus* infection, as revealed using the zebrafish model of infection (40). In particular, extracellular cords, due to their size, prevent the bacilli from being phagocytosed by macrophages and neutrophils, representing an important mechanism of immune evasion (14, 39). We demonstrate here that treatment of infected macrophages was associated with reduced intra- and extracellular cording of the R variant. It is very likely that RFB prevents cording, as a consequence of the inhibition of bacterial replication/killing. Cords are a hallmark of virulence of the R variant of *M. abscessus*, as emphasized by a deletion mutant of *MAB_4780*, encoding a dehydratase, displaying a pronounced defect in cording and a highly attenuated phenotype in macrophages (63). Importantly, we observed also a significant decrease in the number of embryos with cords following RFB treatment in infected zebrafish. It is worth highlighting that in the presence of RFB, there is no change in the number of embryos with cords between 2 and 4 dpi, implying that while RFB does not degrade or modify the bacterial cord structure, it likely prevents the formation of additional cords. Moreover, the effect of RFB on cord reduction is particularly interesting as it may prevent the subsequent formation of abscesses (14), considered as a marker of severity of the disease. Consistent with this hypothesis, a marked decrease in abscess formation was observed in RFB-treated zebrafish embryos. Overall, this work supports the practicality of zebrafish as a pre-clinical model to evaluate in real-time the bactericidal efficacy of RFB against *M. abscessus* infection in the sole context of innate immunity.

In summary, although there is a clear lack of bactericidal activity of drugs against *M. abscessus* (64), these findings support the high activity of RFB against *M. abscessus in vivo* and *in vitro*. Our results further emphasize the efficacy of RFB against both extracellular and intracellular forms of *M. abscessus,* both co-existing in infected patients, as well as a protective effect in an animal model of *M. abscessus* infection. In addition, we have provided further evidence that S and R variants are differentially susceptible to RFB, likely due to the GPL layer, however the MIC values are not predictive of intracellular drug efficacy.

Together with the fact that RFB is an FDA-approved drug that is already used to treat tuberculosis (66) and *M. avium* infections (67) with favourable pharmacological properties (68), our data strengthen the view that RFB should be considered as a repurposing drug candidate for the treatment of *M. abscessus* infections. Importantly, recent work has shown that RFB is synergistic in combinations with other antimicrobials such as clarithromycin, imipenem and tigecycline, and significantly improves the activity of imipenem-tedizolid drug combinations (32, 48, 53, 65). Future studies are required to test whether these RFB combinations are effective against *M. abscessus* pulmonary infections.

ACKNOWLEDGMENTS

MDJ received a post-doctoral fellowship granted by Labex EpiGenMed, an «Investissements d'avenir» program (ANR-10-LABX-12-01). This study was supported by the Association Gregory Lemarchal and Vaincre la Mucoviscidose (RIF20180502320) to LK.

The authors have no conflict of interest to declare.

REFERENCES

1. Johansen MD, Herrmann J-L, Kremer L. 2020. Non-tuberculous mycobacteria and the rise of *Mycobacterium abscessus*. Nat Rev Microbiol. 18:392-407.

2. Cowman S, van Ingen J, Griffith DE, Loebinger MR. 2019. Non-tuberculous mycobacterial pulmonary disease. Eur Respir J 54:1900250.

3. Jönsson BE, Gilljam M, Lindblad A, Ridell M, Wold AE, Welinder-Olsson C. 2007. Molecular epidemiology of *Mycobacterium abscessus*, with focus on cystic fibrosis. J Clin Microbiol 45:1497–1504.

4. Esther CR, Esserman DA, Gilligan P, Kerr A, Noone PG. 2010. Chronic *Mycobacterium abscessus* infection and lung function decline in cystic fibrosis. J Cyst Fibros 9:117–123.

5. Catherinot E, Roux A-L, Macheras E, Hubert D, Matmar M, Dannhoffer L, Chinet T, Morand P, Poyart C, Heym B, Rottman M, Gaillard J-L, Herrmann J-L. 2009. Acute respiratory failure involving an R variant of *Mycobacterium abscessus*. J Clin Microbiol 47:271–274.

6. Adekambi T, Sassi M, van Ingen J, Drancourt M. 2017. Reinstating *Mycobacterium massiliense* and *Mycobacterium bolletii* as species of the *Mycobacterium abscessus* complex. Int J Syst Evol Microbiol 67:2726–2730.

7. Koh W-J, Jeon K, Lee NY, Kim B-J, Kook Y-H, Lee S-H, Park YK, Kim CK, Shin SJ, Huitt GA, Daley CL, Kwon OJ. 2011. Clinical significance of differentiation of *Mycobacterium massiliense* from *Mycobacterium abscessus.* Am J Respir Crit Care Med 183:405–410.

8. Howard ST, Rhoades E, Recht J, Pang X, Alsup A, Kolter R, Lyons CR, Byrd TF. 2006. Spontaneous reversion of *Mycobacterium abscessus* from a smooth to a rough morphotype is associated with reduced expression of glycopeptidolipid and reacquisition of an invasive phenotype. Microbiology (Reading, Engl) 152:1581–1590.

9. Gutiérrez AV, Viljoen A, Ghigo E, Herrmann J-L, Kremer L. 2018. Glycopeptidolipids, a double-edged sword of the *Mycobacterium abscessus* complex. Front Microbiol 9:1145.

10. Roux A-L, Viljoen A, Bah A, Simeone R, Bernut A, Laencina L, Deramaudt T, Rottman M, Gaillard J-L, Majlessi L, Brosch R, Girard-Misguich F, Vergne I, de Chastellier C, Kremer L, Herrmann J-L. 2016. The distinct fate of smooth and rough *Mycobacterium abscessus* variants inside macrophages. Open Biol 6:160185.

11. Bernut A, Viljoen A, Dupont C, Sapriel G, Blaise M, Bouchier C, Brosch R, de Chastellier C, Herrmann J-L, Kremer L. 2016. Insights into the smooth-to-rough transitioning in *Mycobacterium bolletii* unravels a functional Tyr residue conserved in all mycobacterial MmpL family members. Mol Microbiol 99:866–883.

12. Sánchez-Chardi A, Olivares F, Byrd TF, Julián E, Brambilla C, Luquin M. 2011. Demonstration of cord formation by rough *Mycobacterium abscessus* variants: implications for the clinical microbiology laboratory. J Clin Microbiol 49:2293–2295.

13. Nessar R, Reyrat J-M, Davidson LB, Byrd TF. 2011. Deletion of the *mmpL4b* gene in the *Mycobacterium abscessus* glycopeptidolipid biosynthetic pathway results in loss of surface colonization capability, but enhanced ability to replicate in human macrophages and stimulate their innate immune response. Microbiology (Reading, Engl) 157:1187–1195.

14. Bernut A, Herrmann J-L, Kissa K, Dubremetz J-F, Gaillard J-L, Lutfalla G, Kremer L. 2014. *Mycobacterium abscessus* cording prevents phagocytosis and promotes abscess formation. Proc Natl Acad Sci USA 111:E943-952.

15. Park IK, Hsu AP, Tettelin H, Shallom SJ, Drake SK, Ding L, Wu U-I, Adamo N, Prevots DR, Olivier KN, Holland SM, Sampaio EP, Zelazny AM. 2015. Clonal diversification and changes in lipid traits and colony morphology in *Mycobacterium abscessus* clinical isolates. J Clin Microbiol 53:3438–3447.

16. Pawlik A, Garnier G, Orgeur M, Tong P, Lohan A, Le Chevalier F, Sapriel G, Roux A-L, Conlon K, Honoré N, Dillies M-A, Ma L, Bouchier C, Coppée J-Y, Gaillard J-L, Gordon SV, Loftus B, Brosch R, Herrmann JL. 2013. Identification and characterization of the genetic changes responsible for the characteristic smooth-to-rough morphotype alterations of clinically persistent *Mycobacterium abscessus*. Mol Microbiol 90:612–629.

17. Madani A, Ridenour JN, Martin BP, Paudel RR, Abdul Basir A, Le Moigne V, Herrmann J-L, Audebert S, Camoin L, Kremer L, Spilling CD, Canaan S, Cavalier J-F. 2019. Cyclipostins and Cyclophostin analogues as multitarget inhibitors that impair growth of *Mycobacterium abscessus*. ACS Infect Dis 5:1597–1608.

18. Lavollay M, Dubée V, Heym B, Herrmann J-L, Gaillard J-L, Gutmann L, Arthur M, Mainardi J-L. 2014. *In vitro* activity of cefoxitin and imipenem against *Mycobacterium abscessus* complex. Clin Microbiol Infect 20:O297–O300.

19. Nessar R, Cambau E, Reyrat JM, Murray A, Gicquel B. 2012. *Mycobacterium abscessus*: a new antibiotic nightmare. J Antimicrob Chemother 67:810–818.

20. van Ingen J, Boeree MJ, van Soolingen D, Mouton JW. 2012. Resistance mechanisms and drug susceptibility testing of nontuberculous mycobacteria. Drug Resist Updat 15:149–161.

21. Brown-Elliott BA, Nash KA, Wallace RJ. 2012. Antimicrobial susceptibility testing, drug resistance mechanisms, and therapy of infections with nontuberculous mycobacteria. Clin Microbiol Rev 25:545–582.

22. Lopeman R, Harrison J, Desai M, Cox J. 2019. Mycobacterium abscessus: Environmental bacterium turned clinical nightmare. Microorganisms 7:90.

23. Luthra S, Rominski A, Sander P. 2018. The role of antibiotic-target-modifying and antibiotic-modifying enzymes in *Mycobacterium abscessus* drug resistance. Front Microbiol 9:2179.

574 24. Wu M-L, Aziz DB, Dartois V, Dick T. 2018. NTM drug discovery: status, gaps and the way forward.
575 Drug Discov Today 23:1502–1519.

576 25. Griffith DE, Aksamit T, Brown-Elliott BA, Catanzaro A, Daley C, Gordin F, Holland SM, Horsburgh
577 R, Huitt G, Iademarco MF, Iseman M, Olivier K, Ruoss S, von Reyn CF, Wallace RJ, Winthrop K,
578 ATS Mycobacterial Diseases Subcommittee, American Thoracic Society, Infectious Disease
579 Society of America. 2007. An official ATS/IDSA statement: diagnosis, treatment, and prevention
580 of nontuberculous mycobacterial diseases. Am J Respir Crit Care Med 175:367–416.

581 26. Floto RA, Olivier KN, Saiman L, Daley CL, Herrmann J-L, Nick JA, Noone PG, Bilton D, Corris P,
582 Gibson RL, Hempstead SE, Koetz K, Sabadosa KA, Sermet-Gaudelus I, Smyth AR, van Ingen J,
583 Wallace RJ, Winthrop KL, Marshall BC, Haworth CS. 2016. US Cystic Fibrosis Foundation and
584 European Cystic Fibrosis Society consensus recommendations for the management of non-
585 tuberculous mycobacteria in individuals with cystic fibrosis: executive summary. Thorax 71:88–
586 90.

587 27. Daley CL, Iaccarino JM, Lange C, Cambau E, Wallace RJ, Andrejak C, Böttger EC, Brozek J, Griffith
588 DE, Guglielmetti L, Huitt GA, Knight SL, Leitman P, Marras TK, Olivier KN, Santin M, Stout JE,
589 Tortoli E, van Ingen J, Wagner D, Winthrop KL. 2020. Treatment of nontuberculous
590 mycobacterial pulmonary disease: an official ATS/ERS/ESCMID/IDSA clinical practice guideline.
591 Eur Respir J 56:2000535.

592 28. Wallace RJ, Dukart G, Brown-Elliott BA, Griffith DE, Scerpella EG, Marshall B. 2014. Clinical
593 experience in 52 patients with tigecycline-containing regimens for salvage treatment of

Mycobacterium abscessus and *Mycobacterium chelonae* infections. J Antimicrob Chemother 69:1945–1953.

29. Roux A-L, Catherinot E, Soismier N, Heym B, Bellis G, Lemonnier L, Chiron R, Fauroux B, Le Bourgeois M, Munck A, Pin I, Sermet I, Gutierrez C, Véziris N, Jarlier V, Cambau E, Herrmann J-L, Guillemot D, Gaillard J-L, OMA group. 2015. Comparing *Mycobacterium massiliense* and *Mycobacterium abscessus* lung infections in cystic fibrosis patients. J Cyst Fibros 14:63–69.

30. Daniel-Wayman S, Abate G, Barber DL, Bermudez LE, Coler RN, Cynamon MH, Daley CL, Davidson RM, Dick T, Floto RA, Henkle E, Holland SM, Jackson M, Lee RE, Nuermberger EL, Olivier KN, Ordway DJ, Prevots DR, Sacchettini JC, Salfinger M, Sassetti CM, Sizemore CF, Winthrop KL, Zelazny AM. 2019. Advancing translational science for pulmonary nontuberculous mycobacterial infections. A road map for research. Am J Respir Crit Care Med 199:947–951.

31. Aziz DB, Low JL, Wu M-L, Gengenbacher M, Teo JWP, Dartois V, Dick T. 2017. Rifabutin is active against *Mycobacterium abscessus* complex. Antimicrob Agents Chemother. 61:e00155-17.

32. Pryjma M, Burian J, Thompson CJ. 2018. Rifabutin acts in synergy and is bactericidal with frontline *Mycobacterium abscessus* antibiotics clarithromycin and tigecycline, suggesting a potent treatment combination. Antimicrob Agents Chemother 62:e00283-18.

33. Rominski A, Roditscheff A, Selchow P, Böttger EC, Sander P. 2017. Intrinsic rifamycin resistance of *Mycobacterium abscessus* is mediated by ADP-ribosyltransferase MAB_0591. J Antimicrob Chemother 72:376–384.

34. Dick T, Shin SJ, Koh W-J, Dartois V, Gengenbacher M. 2019. Rifabutin is active against *Mycobacterium abscessus* in mice. Antimicrob Agents Chemother 64:e01943-19.

35. Singh S, Bouzinbi N, Chaturvedi V, Godreuil S, Kremer L. 2014. *In vitro* evaluation of a new drug combination against clinical isolates belonging to the *Mycobacterium abscessus* complex. Clin Microbiol Infect 20:O1124-1127.

36. Halloum I, Viljoen A, Khanna V, Craig D, Bouchier C, Brosch R, Coxon G, Kremer L. 2017. Resistance to thiacetazone derivatives active against *Mycobacterium abscessus* involves mutations in the MmpL5 transcriptional repressor MAB_4384. Antimicrob Agents Chemother 61:e02509-16.

37. Woods, GL, Brown-Elliott, BA, Conville, PS, Desmond, EP, Hall, GS, Lin G, Pfyffer GE, Ridderhof, JC, Siddiqi, SH, Wallace, RJ. 2011. Susceptibility testing of mycobacteria, nocardiae and other aerobic actinomycetes: approved standardSecond Edition. M24-A2. Clinical and Laboratory Standards Institute, Wayne, PA 2011.

38. Lamason RL, Mohideen M-APK, Mest JR, Wong AC, Norton HL, Aros MC, Jurynec MJ, Mao X, Humphreville VR, Humbert JE, Sinha S, Moore JL, Jagadeeswaran P, Zhao W, Ning G, Makalowska I, McKeigue PM, O'donnell D, Kittles R, Parra EJ, Mangini NJ, Grunwald DJ, Shriver MD, Canfield VA, Cheng KC. 2005. SLC24A5, a putative cation exchanger, affects pigmentation in zebrafish and humans. Science 310:1782–1786.

631 39. Bernut A, Dupont C, Sahuquet A, Herrmann J-L, Lutfalla G, Kremer L. 2015. Deciphering and
632 imaging pathogenesis and cording of *Mycobacterium abscessus* in zebrafish embryos. J Vis Exp
633 103:e53130.

634 40. Bernut A, Le Moigne V, Lesne T, Lutfalla G, Herrmann J-L, Kremer L. 2014. *In vivo* assessment of
635 drug efficacy against *Mycobacterium abscessus* using the embryonic zebrafish test system.
636 Antimicrob Agents Chemother 58:4054–4063.

637 41. Lefebvre A-L, Dubée V, Cortes M, Dorchêne D, Arthur M, Mainardi J-L. 2016. Bactericidal and
638 intracellular activity of β-lactams against *Mycobacterium abscessus*. J Antimicrob Chemother
639 71:1556–1563.

640 42. Story-Roller E, Maggioncalda EC, Lamichhane G. 2019. Select β-lactam combinations exhibit
641 synergy against *Mycobacterium abscessus in vitro*. Antimicrob Agents Chemother 63:e00614-19.

642 43. Medjahed H, Reyrat J-M. 2009. Construction of *Mycobacterium abscessus* defined
643 glycopeptidolipid mutants: comparison of genetic tools. Appl Environ Microbiol 75:1331–1338.

644 44. Roux A-L, Ray A, Pawlik A, Medjahed H, Etienne G, Rottman M, Catherinot E, Coppée J-Y, Chaoui
645 K, Monsarrat B, Toubert A, Daffé M, Puzo G, Gaillard J-L, Brosch R, Dulphy N, Nigou J, Herrmann
646 J-L. 2011. Overexpression of proinflammatory TLR-2-signalling lipoproteins in hypervirulent
647 mycobacterial variants. Cell Microbiol 13:692–704.

648 45. Ripoll F, Pasek S, Schenowitz C, Dossat C, Barbe V, Rottman M, Macheras E, Heym B, Herrmann
649 J-L, Daffé M, Brosch R, Risler J-L, Gaillard J-L. 2009. Non mycobacterial virulence genes in the
650 genome of the emerging pathogen *Mycobacterium abscessus*. PLoS ONE 4:e5660.

651 46. Balganesh M, Dinesh N, Sharma S, Kuruppath S, Nair AV, Sharma U. 2012. Efflux pumps of
652 *Mycobacterium tuberculosis* play a significant role in antituberculosis activity of potential drug
653 candidates. Antimicrob Agents Chemother 56:2643–2651.

654 47. Dupont C, Viljoen A, Thomas S, Roquet-Banères F, Herrmann J-L, Pethe K, Kremer L. 2017.
655 Bedaquiline inhibits the ATP synthase in *Mycobacterium abscessus* and is effective in infected
656 zebrafish. Antimicrob Agents Chemother 61:e01225-17.

657 48. Cheng A, Tsai Y-T, Chang S-Y, Sun H-Y, Wu U-I, Sheng W-H, Chen Y-C, Chang S-C. 2019. *In vitro*
658 synergism of rifabutin with clarithromycin, imipenem, and tigecycline against the
659 *Mycobacterium abscessus* complex. Antimicrob Agents Chemother 63:e02234-18.

660 49. Luna-Herrera J, Reddy MV, Gangadharam PRJ. 1995. *In vitro* and intracellular activity of rifabutin
661 on drug-susceptible and multiple drug-resistant (MDR) tubercle bacilli. J Antimicrob Chemother
662 36:355–363.

663 50. Dubée V, Bernut A, Cortes M, Lesne T, Dorchene D, Lefebvre A-L, Hugonnet J-E, Gutmann L,
664 Mainardi J-L, Herrmann J-L, Gaillard J-L, Kremer L, Arthur M. 2015. β-Lactamase inhibition by
665 avibactam in *Mycobacterium abscessus*. J Antimicrob Chemother 70:1051–1058.

666 51. Baysarowich J, Koteva K, Hughes DW, Ejim L, Griffiths E, Zhang K, Junop M, Wright GD. 2008.
667 Rifamycin antibiotic resistance by ADP-ribosylation: Structure and diversity of Arr. Proc Natl
668 Acad Sci USA 105:4886–4891.

669 52. Ganapathy US, Dartois V, Dick T. 2019. Repositioning rifamycins for *Mycobacterium abscessus*
670 lung disease. Expert Opin Drug Discov 1–12.

671 53. Le Run E, Arthur M, Mainardi J-L. 2018. *In vitro* and intracellular activity of imipenem combined
672 with rifabutin and avibactam against *Mycobacterium abscessus*. Antimicrob Agents Chemother
673 62:e00623-18.

674 54. Brambilla C, Llorens-Fons M, Julián E, Noguera-Ortega E, Tomàs-Martínez C, Pérez-Trujillo M,
675 Byrd TF, Alcaide F, Luquin M. 2016. Mycobacteria clumping increase their capacity to damage
676 macrophages. Front Microbiol 7:1562.

677 55. Jagielski T, Bakuła Z, Brzostek A, Minias A, Stachowiak R, Kalita J, Napiórkowska A,
678 Augustynowicz-Kopeć E, Żaczek A, Vasiliauskiene E, Bielecki J, Dziadek J. 2018. Characterization
679 of mutations conferring resistance to rifampin in *Mycobacterium tuberculosis* clinical strains.
680 Antimicrob Agents Chemother 62:e01093-18.

681 56. Richard M, Gutiérrez AV, Viljoen AJ, Ghigo E, Blaise M, Kremer L. 2018. Mechanistic and
682 structural insights into the unique TetR-dependent regulation of a drug efflux pump in
683 *Mycobacterium abscessus*. Front Microbiol 9:649.

684 57. Richard M, Gutiérrez AV, Viljoen A, Rodriguez-Rincon D, Roquet-Baneres F, Blaise M, Everall I,
685 Parkhill J, Floto RA, Kremer L. 2019. Mutations in the MAB_2299c TetR regulator confer cross-
686 resistance to clofazimine and bedaquiline in *Mycobacterium abscessus*. Antimicrob Agents
687 Chemother 63:e01316-18.

688 58. Gutiérrez AV, Richard M, Roquet-Banères F, Viljoen A, Kremer L. 2019. The TetR-family
689 transcription factor MAB_2299c regulates the expression of two distinct MmpS-MmpL efflux

690 pumps involved in cross-resistance to clofazimine and bedaquiline in *Mycobacterium abscessus*.
691 Antimicrob Agents Chemother. 63:e01000-19.

692 59. Koteva K, Cox G, Kelso JK, Surette MD, Zubyk HL, Ejim L, Stogios P, Savchenko A, Sørensen D,
693 Wright GD. 2018. Rox, a rifamycin resistance enzyme with an unprecedented mechanism of
694 action. Cell Chemical Biology 25:403-412.e5.

695 60. Lefebvre A-L, Le Moigne V, Bernut A, Veckerlé C, Compain F, Herrmann J-L, Kremer L, Arthur M,
696 Mainardi J-L. 2017. Inhibition of the β-lactamase BlaMab by avibactam improves the *in vitro* and
697 *in vivo* efficacy of imipenem against *Mycobacterium abscessus*. Antimicrob Agents Chemother
698 61:e02440-16.

699 61. Marshall VP, Cialdella JI, Ohlmann GM, Gray GD. 1983. MIC values do not predict the
700 intraphagocytic killing of *Staphylococcus aureus* by naphthalenic ansamycins. J Antibiot
701 36:1549–1560.

702 62. Viljoen A, Viela F, Kremer L, Dufrêne YF. 2020. Fast chemical force microscopy demonstrates
703 that glycopeptidolipids define nanodomains of varying hydrophobicity on mycobacteria.
704 Nanoscale Horiz 5:944–953.

705 63. Halloum I, Carrère-Kremer S, Blaise M, Viljoen A, Bernut A, Le Moigne V, Vilchèze C, Guérardel Y,
706 Lutfalla G, Herrmann J-L, Jacobs WR, Kremer L. 2016. Deletion of a dehydratase important for
707 intracellular growth and cording renders rough *Mycobacterium abscessus* avirulent. Proc Natl
708 Acad Sci USA 113:E4228-4237.

64. Maurer FP, Bruderer VL, Ritter C, Castelberg C, Bloemberg GV, Böttger EC. 2014. Lack of antimicrobial bactericidal activity in *Mycobacterium abscessus.* Antimicrob Agents Chemother 58:3828–3836.

65. Le Run E, Arthur M, Mainardi J-L. 2019. *In vitro* and intracellular activity of imipenem combined with tedizolid, rifabutin, and avibactam against *Mycobacterium abscessus.* Antimicrob Agents Chemother 63:e01915-18.

66. Lee H, Ahn S, Hwang NY, Jeon K, Kwon OJ, Huh HJ, Lee NY, Koh W-J. 2017. Treatment outcomes of rifabutin-containing regimens for rifabutin-sensitive multidrug-resistant pulmonary tuberculosis. Int J Infect Dis 65:135–141.

67. Griffith DE. 2018. Treatment of *Mycobacterium avium* complex (MAC). Semin Respir Crit Care Med 39:351–361.

68. Blaschke TF, Skinner MH. 1996. The clinical pharmacokinetics of rifabutin. Clin Infect Dis 22 Suppl 1:S15-21; discussion S21-22.

Table 1. Drug susceptibility/resistance profile of smooth and rough variants derived from the reference *M. abscessus* 104536^{T} strain to various rifamycins in CaMBH. MIC (µg/mL) were determined following the CLSI guidelines.

Strain	Morphotype	MIC (µg/mL)			
		RFB	**RIF**	**RPT**	**RFX**
CIP104536 (S)	S	64	>128	>128	>128
CIP104536 (R)	R	16	>128	>128	>128
ΔMAB_mmpL4b	R	16	>128	>128	>128
ΔMAB_mmpL4b_C	S	32	>128	>128	>128
CIP104536 (S) + pMV306-*MAB_1409c-HA*	S	64	>128	>128	>128
CIP104536 (R) + pMV306-*MAB_1409c-HA*	R	64	>128	>128	>128

RFB, Rifabutin; RIF, rifampicin; RPT, rifapentine; RFX, rifaximin.

Table 2. Comparison of the activity of RFB against clinical isolates from CF and non-CF patients. The MIC (µg/mL) was determined in Cation-Adjusted Mueller-Hinton broth for different subspecies belonging to the *M. abscessus* complex. Results are from 3 independent experiments. RFB, rifabutin.

Strain	Morphotype	Source	RFB
M. abscessus			
CIP104536	S	Non-CF	50
3321	S	Non-CF	50
1298	S	CF	50
2587	S	CF	100
2069	S	Non-CF	100
CF	S	CF	25
2524	R	CF	25
2648	R	CF	25
3022	R	Non-CF	50
5175	R	CF	25
CIP104536	R	Non-CF	25
M. massiliense			
CIP108297	R	Addison Disease	50
210	R	CF	100
179	R	CF	100
CIP108297	S	Addison Disease	100
140	S	CF	50
185	S	CF	100
107	S	CF	50
122	S	CF	100
120	S	CF	6.25
212	S	CF	100
100	S	CF	100
111	S	CF	100
M. bolletii			
CIP108541	S	Non reported	100
114	S	CF	100
17	S	CF	50
116	S	CF	100
97	S	CF	100
112	R	CF	100
19	R	Non-CF	50
10	R	Non reported	100
108	R	CF	25

747 **Table 3. Characterisitics of spontaneous RFB-resistant mutants of *M. abscessus*.** MIC (µg/mL) were
748 determined in Cation-adjusted Mueller-Hinton broth. Resistant strains were derived from the rough
749 *M. abscessus* CIP104536^T parental strain on Middlbrook 7H10 supplemented with either 25 or 50
750 µg/mL RFB. Single nucleotide polymorphism identification in *rpoB* (*MAB_3869c)* and corresponding
751 amino acid changes are also indicated. RFB, rifabutin.
752

753

	MIC (µg/ml)	Mutation in *rpoB*	
		SNP	AA change
CIP104536^T (R)	12.5	-	-
25.1	50	C1339T	H447Y
25.2	100	C1339G	H447D
50.1	50	C1339T	H447Y
50.2	50	C1355T	S452L

754 **FIGURE LEGENDS**

755 **Figure 1. *In vitro* activity of rifabutin.** *M. abscessus* CIP104536^T S (left panel) or R (right panel) was
756 exposed either to 200, 100, 50, 25, 12.5 or 6.25 µg/mL RFB or 16 µg/mL IPM in CaMHB at 30°C. At
757 various time points, bacteria were plated on LB agar and further incubated at 30°C for 4 days prior to
758 CFU counting. Results are expressed as the mean of triplicates ± SD and are representative of two
759 independent experiments. *$P \leq 0.05$, ** $P \leq 0.01$.

760

761 **Figure 2. Intracellular activity of RFB on *M. abscessus*-infected THP-1 cells**. **(A)** Macrophages were
762 infected with *M. abscessus* S-morphotype and **(B)** R-morphotype expressing tdTomato (MOI of 2:1)
763 for 3 hrs prior to treatment with RIF (50 µg/mL), AMK (50 µg/mL), RFB (12.5 µg/mL) or DMSO. CFU
764 were determined at 0, 1 and 3 dpi. Data are mean values ± SD for three independent experiments.
765 Data were analysed using a one-way ANOVA Kruskal-Wallis test. **(C)** Percentage of infected THP-1
766 macrophages at 0, 1 and 3 days post-infection after infection with *M. abscessus* S or **(D)** *M. abscessus*
767 R. Data are mean values ± SD for three independent experiments. Data were analysed using a one-
768 way ANOVA Kruskal-Wallis test. **(E)** Percentage of S-infected macrophage categories and **(F)**
769 percentage of R-infected macrophage categories infected with different numbers of bacilli (<5 bacilli;
770 5-10 bacilli and >10 bacilli). The categories were counted at 0 or at 1 and 3 days post-infection in the
771 absence of antibiotics or in the presence of RIF or AMK at 50 µg/mL, or RFB at 12.5 µg/mL. Values are
772 means ± SD from three independent experiments performed in triplicate. **(G)** Four immuno-
773 fluorescent fields were taken at 1 day post-infection showing macrophages infected with *M.*
774 *abscessus* expressing Tdtomato (red). The surface and the endolysosomal system of the macrophages
775 were detected using anti-CD63 antibodies (green). The nuclei were stained with DAPI (blue). White
776 arrows indicate individual or aggregate mycobacteria. Scale bar, 20 µm. ** $P \leq 0.01$, *** $P \leq 0.001$.

777

778 **Figure 3. Intracellular activity of RFB on S and R clinical isolates.** CFU counts of clinical isolates
779 exposed to 25 and 12.5 µg/mL RFB. Macrophages were infected with *M. abscessus* **(A-B)** *M. bolletii*
780 **(C-D)** or *M. massiliense* **(E-G)** clinical strains belonging to S or R morphotypes at MOI of 2:1 for 3 hrs
781 prior to treatment with 250 µg/mL AMK for 2 hrs to kill extracellular bacteria. Following extensive
782 PBS washes, cells were exposed to 50 µg/mL RIF, 50 µg/mL AMK, 25 or 12.5 µg/mL RFB . CFU were

783 determined at 0, 1 and 3 days post-infection. Data are mean values ± SD for two independent
784 experiments. Data were analysed using the *t*-test. *$P \leq 0.05$, ** $P \leq 0.01$, *** $P \leq 0.001$.
785
786 **Figure 4. Activity of RFB on extracellular and intracellular cords. (A)** Total number of cords
787 displayed in 20 fields at 3 days post-infection after infection of macrophages with *M. abscessus* R
788 variant. Data are mean values ± SD for three independent experiments performed in triplicate. Data
789 were analysed using one tailed Mann Whitney's *t*-test. **(B)** Percentage of cords formed either
790 extracellularly or intracellularly. The two categories were counted at 3 days post-infection in the
791 absence of antibiotics or in the presence of 50 µg/mL RIF, 50 µg/mL AMK or 12.5 µg/mL RFB.
792 Extracellular or intracellular cords are highlighted using the indicated colour codes. Values are means
793 ± SD for two independent experiments performed each time in triplicate. **(C)** Four immuno-
794 fluorescent fields were taken at 3 days post-infection showing the cords formed extracellularly or
795 within macrophages infected with *M. abscessus* R variant expressing Tdtomato (red). Macrophages
796 were infected for 3 days in the presence of DMSO, RIF (50 µg/mL), AMK (50 µg/mL) or RFB (12.5
797 µg/mL). The macrophage surface was stained using anti-CD63 antibodies (green). The nuclei were
798 stained with DAPI (blue). White arrows indicate intracellular cords, while red arrows indicate
799 extracellular cords. Scale bars represent 20 µm. Results represent the average of a total of 120 fields
800 per condition. **** $P \leq 0.0001$.
801
802 **Figure 5. RFB displays high bactericidal activity against *M. abscessus* in an embryonic zebrafish**
803 **infection model. (A)** Groups of uninfected embryos were immersed in water containing increasing
804 concentrations of RFB (ranging from 3.125 to 250 µg/mL) for 4 days. The red bar indicates the
805 duration of treatment. The graph shows the survival of the RFB-treated and untreated (DMSO)
806 embryos over a 12-days period. **(B)** Zebrafish embryos at 30 hrs post-fertilisation were intravenously
807 infected with approximately 250-300 CFU of *M. abscessus* CIP104536^T (R variant) expressing
808 tdTomato (n=20-25). A standard PBS injection control was included for each experiment. At 1 dpi,
809 embryos were randomly split into equal groups of approximately 20 embryos per group, and varying
810 concentrations of RFB (5 to 50 µg/mL) were added to the water. DMSO was included as a positive
811 control group. RFB was changed daily after which, embryos were washed twice in fresh embryo
812 water, maintained in embryo water and monitored daily over a 12-days period. Each treatment group

was compared against the untreated infected group with significant differences calculated using the log-rank (Mantel-Cox) statistical test for survival curves. Data shown is the merge of three independent experiments **(C)** Bacterial burden was determined at 2, 4 and 6 days post-infection following treatment with either DMSO or 50 µg/mL RFB. Bacteria were quantified by fluorescent pixel count determination using ImageJ software, with each data point representing a single embryo. Error bars represent standard deviations. Statistical significance was determined by Student's *t*-test. The plots represent a pool of 2 independent experiments containing approximately 20-25 embryos per group. **(D)** Representative embryos from the untreated group (WT) (upper panel) and from the treated group with 50 µg/mL RFB at 6 days post-infection. White arrowheads show tdTomato-expressing bacteria. Scale bars represent 1 mm. *$P \leq 0.05$, *** $P \leq 0.001$, **** $P \leq 0.0001$.

Figure 6. RFB reduces the pathophysiological traits of *M. abscessus* infection in zebrafish embryos. **(A)** Proportion of embryos with cords at 2 and 4 days post-infection in infected embryos that were either untreated or treated with 50 µg/mL RFB (250-300 CFU, n=30). Data were analysed using an unpaired student's *t*-test. Data shown is the mean of three independent experiments ± SD. **(B)** Total percentage of embryos with abscesses at 4 and 6 dpi in infected embryos that were either untreated or treated with 50 µg/mL RFB (250-300 CFU, n=30). Data were analysed using an unpaired student's *t*-test. Data shown is the mean of three independent experiments ± SD. **(C-D)** Representative zebrafish images of untreated (WT) embryos and those treated with treated with 50 µg/mL RFB at 6 dpi. Scale bar represents 0.5 mm. White arrows indicate extracellular cords. The white box highlights a large extracellular cord based on the size and morphology, with the scale bar representing 100 µm. Red overlay represents *M. abscessus* expressing tdTomato. *$P \leq 0.05$.

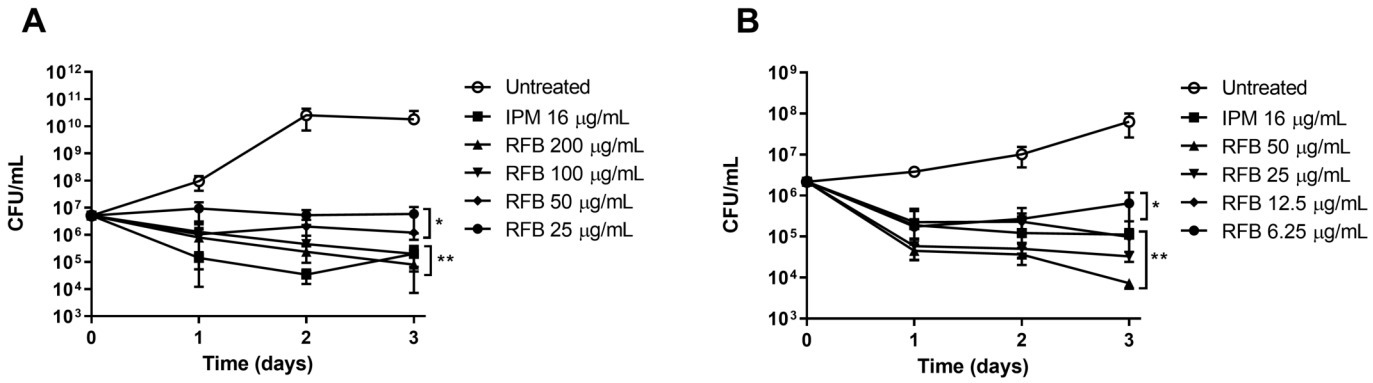
A
CFU/mL
Time (days)
Untreated
IPM 16 μg/mL
RFB 200 μg/mL
RFB 100 μg/mL
RFB 50 μg/mL
RFB 25 μg/mL
*
**
B
CFU/mL
Time (days)
Untreated
IPM 16 μg/mL
RFB 50 μg/mL
RFB 25 μg/mL
RFB 12.5 μg/mL
RFB 6.25 μg/mL
*
**

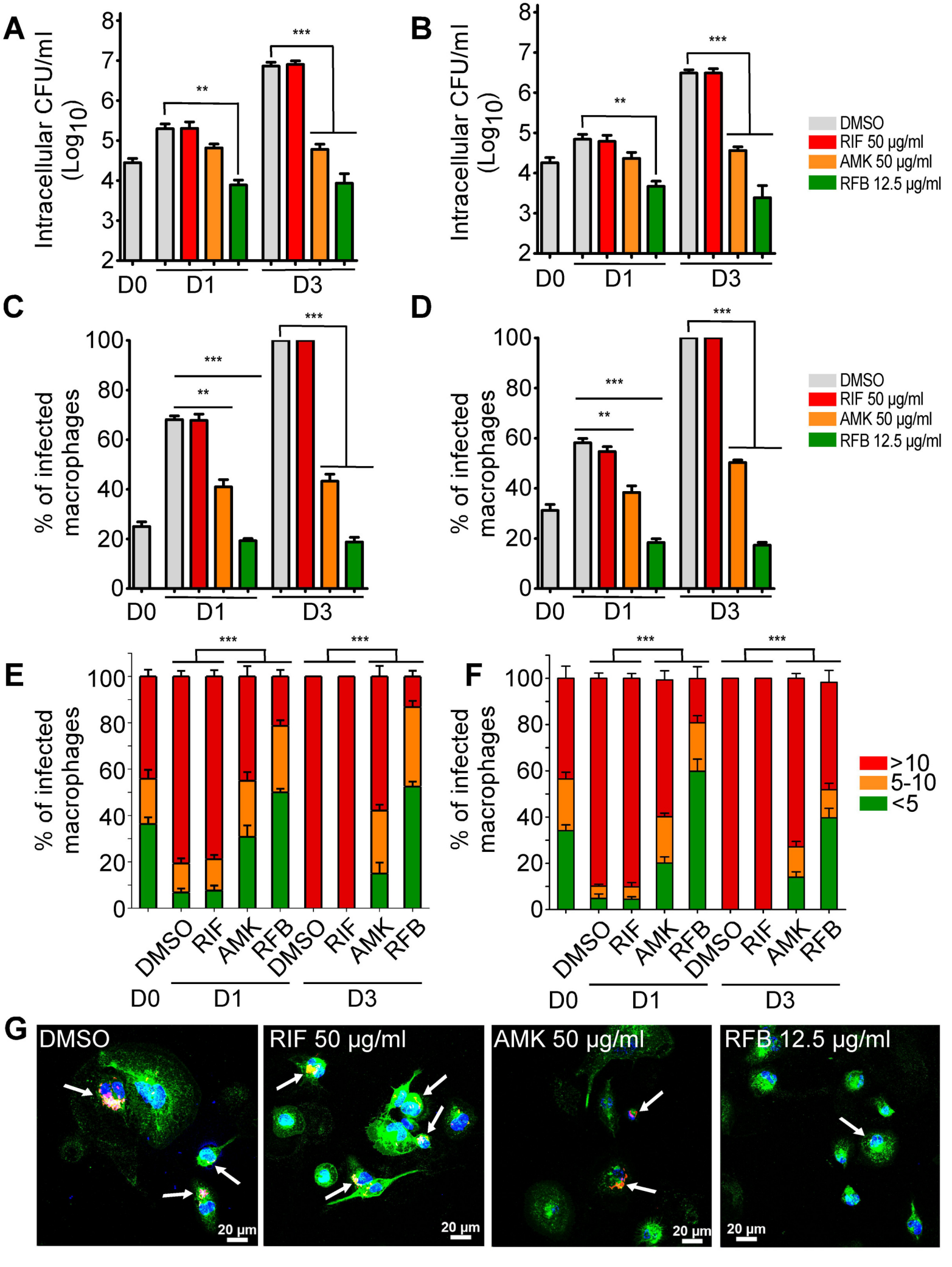
A
Intracellular CFU/ml (Log10)
8
7
6
5
4
3
2
**
***
D0
D1
D3
B
Intracellular CFU/ml (Log10)
8
7
6
5
4
3
2
**
***
D0
D1
D3
DMSO
RIF 50 µg/ml
AMK 50 µg/ml
RFB 12.5 µg/ml
C
% of infected macrophages
100
80
60
40
20
0
***
**
D0
D1
D3
D
% of infected macrophages
100
80
60
40
20
0
***
**
D0
D1
D3
DMSO
RIF 50 µg/ml
AMK 50 µg/ml
RFB 12.5 µg/ml
E
% of infected macrophages
100
80
60
40
20
0
***
***
DMSO
RIF
AMK
RFB
DMSO
RIF
AMK
RFB
D0
D1
D3
F
% of infected macrophages
100
80
60
40
20
0
***
***
DMSO
RIF
AMK
RFB
DMSO
RIF
AMK
RFB
D0
D1
D3
>10
5-10
<5
G
DMSO
RIF 50 µg/ml
AMK 50 µg/ml
RFB 12.5 µg/ml
20 µm
20 µm
20 µm
20 µm

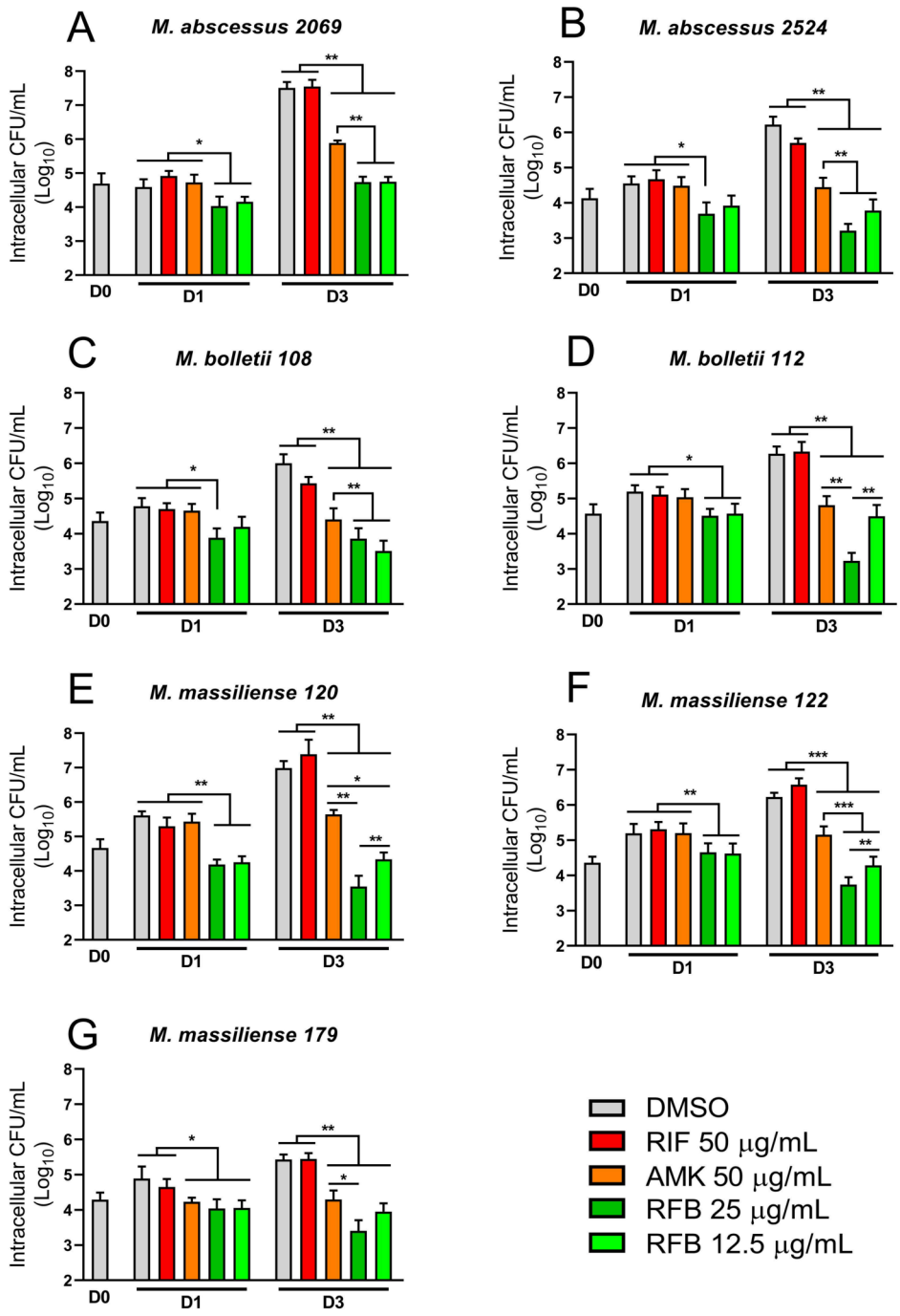
A
M. abscessus 2069
B
M. abscessus 2524
C
M. bolletii 108
D
M. bolletii 112
E
M. massiliense 120
F
M. massiliense 122
G
M. massiliense 179
Intracellular CFU/mL (Log10)
D0
D1
D3
DMSO
RIF 50 μg/mL
AMK 50 μg/mL
RFB 25 μg/mL
RFB 12.5 μg/mL

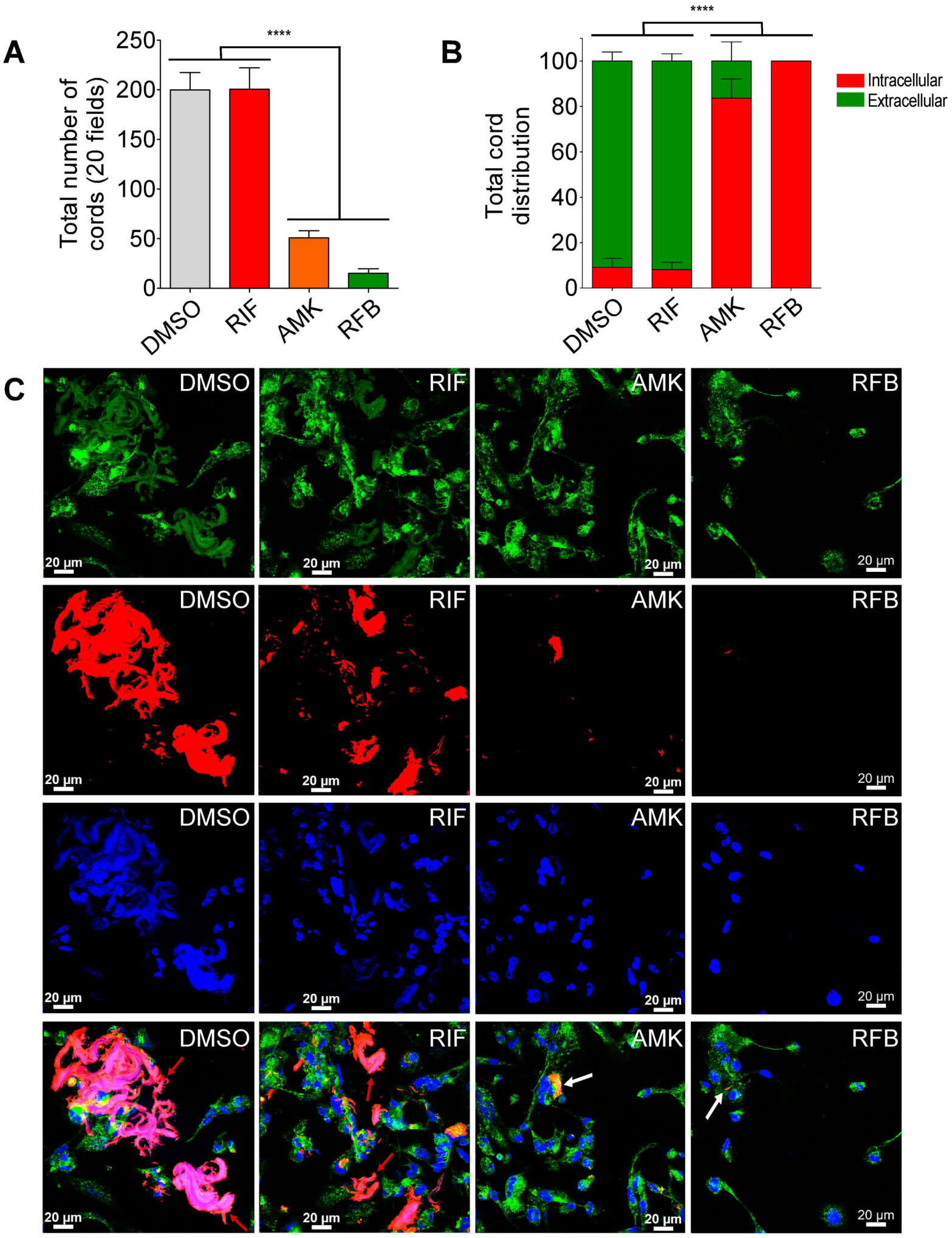
A
Total number of cords (20 fields)
250
200
150
100
50
0
****
DMSO
RIF
AMK
RFB
B
Total cord distribution
100
80
60
40
20
0
****
Intracellular
Extracellular
DMSO
RIF
AMK
RFB
C
DMSO
RIF
AMK
RFB
20 µm

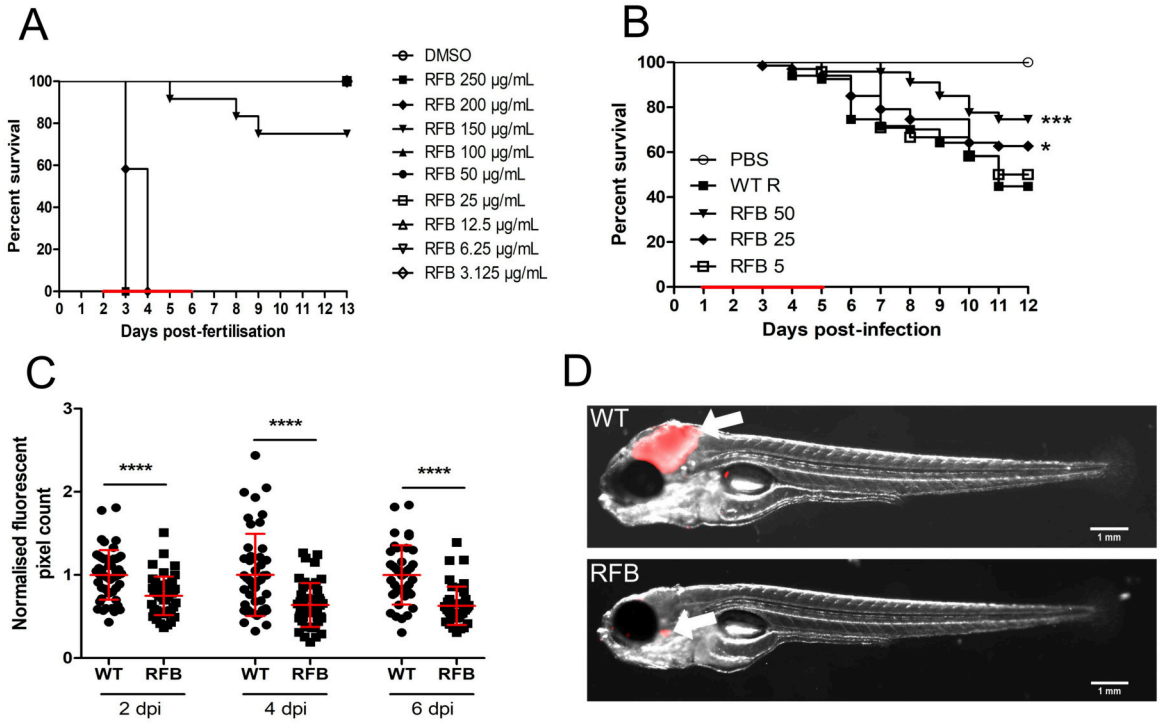
A
Percent survival
Days post-fertilisation
DMSO
RFB 250 µg/mL
RFB 200 µg/mL
RFB 150 µg/mL
RFB 100 µg/mL
RFB 50 µg/mL
RFB 25 µg/mL
RFB 12.5 µg/mL
RFB 6.25 µg/mL
RFB 3.125 µg/mL
B
Percent survival
Days post-infection
PBS
WT R
RFB 50
RFB 25
RFB 5
***
*
C
Normalised fluorescent pixel count
****
****
****
WT
RFB
2 dpi
4 dpi
6 dpi
D
WT
RFB
1 mm
1 mm

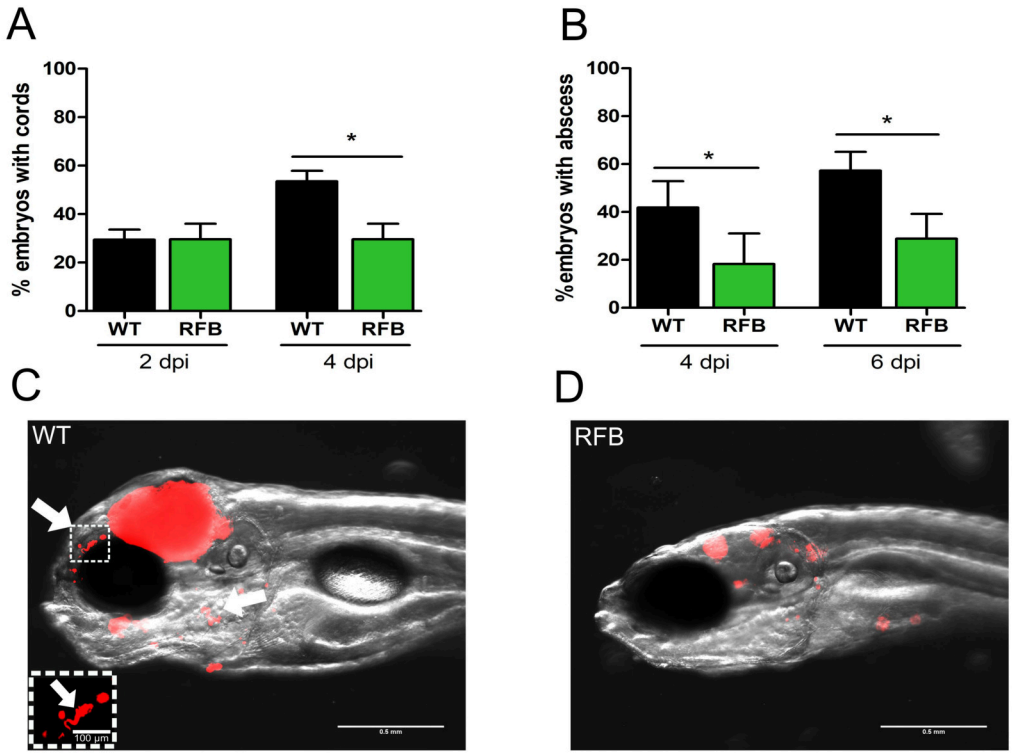
A
% embryos with cords
100
80
60
40
20
0
*
WT
RFB
WT
RFB
2 dpi
4 dpi
B
%embryos with abscess
100
80
60
40
20
0
*
*
WT
RFB
WT
RFB
4 dpi
6 dpi
C
WT
100 µm
0.5 mm
D
RFB
0.5 mm